TOPLHC NOTE

ATLAS-CONF-2013-102
CMS PAS TOP-13-005

September 15, 2013

Combination of ATLAS and CMS results on the mass of the top-quark using up to 4.9 fb^{-1} of $\sqrt{s} = 7$ TeV LHC data

The ATLAS and CMS Collaborations

Abstract

A combination of top-quark mass measurements performed by the ATLAS and CMS experiments at the LHC is presented. The datasets used correspond to an integrated luminosity per experiment of up to 4.9 fb^{-1} of proton-proton collisions at a centre-of-mass energy of 7 TeV. The combination includes measurements in the $t\bar{t} \to$ lepton+jets, $t\bar{t} \to$ di-lepton and $t\bar{t} \to$ all jets channels. The resulting combined LHC measurement of the top-quark mass is $m_{\mathrm{top}} = 173.29 \pm 0.23$ (stat) $\pm$ 0.92 (syst) GeV, with a total uncertainty of 0.95 GeV.

1 Introduction

The top-quark mass (m_{top}) is an important parameter of the Standard Model of particle physics (SM). Precise m_{top} measurements are critical inputs to global electroweak fits [1], provide constraints on the properties of the Higgs boson, and help in assessing the internal consistency of the SM and of its extensions.

At the Tevatron a large number of measurements of m_{top} have been performed by CDF and D0 based on Run I and Run II data for integrated luminosities ($\mathcal{L}_{\text{int}}$) of up to 8.7 fb^{-1}. To increase the precision on the experimental knowledge of this parameter, a combination of the individual results has been performed. The present Tevatron m_{top} combination yields $m_{\text{top}} = 173.20 \pm 0.51$ (stat) $\pm$ 0.71 (syst) GeV = 173.20 $\pm$ 0.87 GeV [2].

Recently, measurements of m_{top} from the LHC experiments have become available. The first LHC m_{top} combination used data from both the 2010 and 2011 proton-proton LHC runs at a centre-of-mass energy of $\sqrt{s} = 7$ TeV, and resulted in $m_{\text{top}} = 173.3 \pm 0.5$ (stat) $\pm$ 1.3 (syst) GeV = 173.3 $\pm$ 1.4 GeV [3].

This note describes an updated LHC m_{top} combination using preliminary and published LHC top-quark mass measurements. Five measurements of m_{top} are used, all based on the LHC $\sqrt{s} = 7$ TeV proton-proton data recorded in 2011. For ATLAS these are comprised of m_{top} results obtained in the $t\bar{t} \to$ lepton+jets and the $t\bar{t} \to$ di-lepton channels using $\mathcal{L}_{\text{int}} = 4.7$ fb^{-1} of data [4, 5]. For CMS, m_{top} measurements from datasets including up to $\mathcal{L}_{\text{int}} = 4.9$ fb^{-1}, in the $t\bar{t} \to$ lepton+jets, $t\bar{t} \to$ di-lepton and $t\bar{t} \to$ all jets channels are used [6–8]. Alternative analysis techniques [9, 10] have recently become available but are not included in the present result.

This document is organised as follows: after a short description of the methodology used for the combination in Section 2, a brief overview of the input measurements is given in Section 3. Details of the mapping between ATLAS and CMS uncertainty classes, and their corresponding correlations are described in Section 4. The results of the m_{top} combination are presented in Section 5, followed, in Section 6, by a discussion of their dependence on the choice of the uncertainty categorisation and on the assumed correlations. Finally, the summary and conclusions are given in Section 7.

2 Methodology

The combination is performed using the Best Linear Unbiased Estimate (BLUE) method [11, 12]. BLUE optimises the coefficients to be used in a linear combination of the input measurements by minimising the total uncertainty of the combined result. In the algorithm, both statistical and systematic uncertainties, as well as the correlations of systematic sources between input measurements, are taken into account, under the hypothesis that all uncertainties are distributed as Gaussians. A realistic evaluation of the correlations is performed and the impact of the various assumptions on the final result is carefully evaluated.

3 Input measurements

The input measurements used for this m_{top} combination correspond to two preliminary ATLAS results in the $t\bar{t} \to$ lepton+jets and $t\bar{t} \to$ di-lepton channels [4, 5], and three published results from the CMS collaboration in the $t\bar{t} \to$ lepton+jets, $t\bar{t} \to$ di-lepton, and $t\bar{t} \to$ all jets channels [6–8].

3.1 ATLAS measurements

The input m_{top} measurements from ATLAS are obtained with various implementations of the template method. Simulated distributions (templates) are constructed for a chosen quantity sensitive to the physics parameter under study, using a number of discrete values of that parameter. The templates are fitted to analytical functions that interpolate between different input values of the physics parameter, which are used in a maximum likelihood fit to the observed data distribution.

In the $t\bar{t} \rightarrow$ lepton+jets analysis, the event reconstruction is performed using a kinematical fit to the $t\bar{t}$ decay hypothesis. A three-dimensional template method is used, where m_{top} is determined simultaneously with a global jet energy scale factor (JSF) exploiting the invariant mass distributions of the hadronically decaying W boson ($t \rightarrow Wb$; $W \rightarrow jj$), and a global b-to-light quark energy scale factor (bJSF). The JSF (bJSF) accounts for possible data-to-simulation differences of the light quark jet energy scale (relative b-to-light quark jet energy scale), mitigating the corresponding systematic uncertainties [4]. No prior knowledge of the uncertainty related to the light- and b-quark jet energy scales is used when determining the JSF and the bJSF.

The $t\bar{t} \rightarrow$ di-lepton analysis is based on a one-dimensional template method, where templates are constructed for the m_{lb} observable, defined as the per event average invariant mass of the charged lepton and the b-quark associated to the top-quarks decay [5].

3.2 CMS measurements

The CMS input measurements in the $t\bar{t} \rightarrow$ lepton+jets [6] and $t\bar{t} \rightarrow$ all jets [8] channels are based on the ideogram method, and employ a kinematic fit of the decay products to a $t\bar{t}$ hypothesis. Likelihood functions for each event (ideograms) that depend on the top-quark mass only or on both the top-quark mass and a JSF are exploited. The ideograms reflect the compatibility of the kinematics of the event with a given decay hypothesis. For the $t\bar{t} \rightarrow$ lepton+jets analysis m_{top} is derived simultaneously with a JSF from $t \rightarrow Wb$ ($W \rightarrow jj$) decays (two-dimensional ideogram method); whereas for the $t\bar{t} \rightarrow$ all jets analysis only m_{top} is obtained from a fit to the data (one-dimensional ideogram method). Similarly to the ATLAS $t\bar{t} \rightarrow$ lepton+jets analysis, no prior knowledge of the jet energy scale uncertainty is used for the determination of the JSF.

For the CMS $t\bar{t} \rightarrow$ di-lepton analysis, the top-quark mass is obtained from an analytical matrix weighting technique, where the full reconstruction of the event kinematics is done under different m_{top} assumptions. For each event, the preferred top-quark mass hypothesis, fulfilling $t\bar{t}$ kinematical constraints, is obtained by assigning weights, that are based on charged lepton energy probability density functions taken from simulation, to the different solutions of the kinematical equations [7].

3.3 Measurements calibration

In all measurements considered in the present combination, the fitting procedures are calibrated to the Monte Carlo (MC) top-quark mass definition. The baseline MC program for the simulation and calibration of the top-quark mass analyses in ATLAS is PowHeg interfaced with Pythia for the parton shower and underlying event modelling [13–15]; MadGraph interfaced with Pythia is used within CMS [14, 16]. The parton configurations generated by MadGraph are matched with the parton showers using the MLM prescriptions [17]. It is expected that the difference between the MC mass definition and the top-quark pole mass is of order 1 GeV [18]. A systematic uncertainty, ranging from 0.02 GeV to 0.20 GeV, depending on the analysis, is assigned to the input measurements, covering differences between MC models.

4 Mapping of uncertainty categories

In this section, the mapping of ATLAS and CMS m_{top} uncertainty categories and their assumed correlations are described. The categorisations outlined in Ref. [3] have been refined and improved using multiple Jet Energy Scale (JES) uncertainty components [19–22]. This allows a better treatment of the correlation assumptions between measurements within the same experiment and of those components that are correlated across experiments. In the following, ρ_{exp} indicates the assumed correlation between measurements from the same experiment, while ρ_{LHC} refers to the assumed correlation between measurements across experiments.

When comparing individual m_{top} input measurements, the quoted systematic uncertainty stemming from corresponding model, detector, or physics effects, could differ for many reasons. Analysis specific details, for example the amount of information exploited for the determination of the event kinematics, and the level of sophistication inherent to the $t\bar{t}$ reconstruction algorithms, can influence the sensitivity of the input measurements to specific signal modelling systematic uncertainties. Similarly, differences in the analysis fitting procedures, for example the possibility to simultaneously determine global jet energy scale factors and m_{top}, can result in a mitigation of the JES related systematic uncertainties. This can yield, in addition, a reduction of some signal modelling systematics, but can also be possibly accompanied by an increase of some detector related uncertainties. Finally, the detector performance can differ due to the experimental specifications: for example a more pronounced dependence of the JES uncertainty on the jet p_T can result in a larger JES component of the m_{top} uncertainty, even for analyses implementing in-situ $t \to Wb,\ W \to jj$ calibration techniques.

For all input measurements, systematic uncertainties are evaluated by varying the respective quantities by ± 1 standard deviation, or by changing the signal model parameters with respect to the default analysis. For each uncertainty component, the observed m_{top} shift with respect to the nominal analysis is used to determine the corresponding top-quark mass uncertainty. For each input m_{top} measurement, the total uncertainty is calculated as the quadratic sum of all individual contributions, *i.e.* neglecting possible correlations between different uncertainty classes and non-linearities in the effect on the measured value of m_{top}.

For the present m_{top} combination, the uncertainty classes and their assumed correlations are summarised in Table 1, and detailed below. The stability of the result under different assumptions is discussed in Section 6.

iJES: This is the part of the JES uncertainty of the m_{top} measurements which originates from in-situ $t\bar{t}$ ($t \to Wb, W \to jj$) calibration procedures and, being statistical in nature, is uncorrelated among the to-be-combined measurements. For analyses performing an in-situ jet calibration based on the simultaneous fit of the reconstructed W boson and top-quark invariant masses, this corresponds to the additional statistical uncertainty associated with the simultaneous determination of a JSF using the $W \to jj$ invariant mass and m_{top} [4, 6]. For the ATLAS $t\bar{t} \to$ lepton+jets measurement [4], it also includes the extra statistical component due to the simultaneous determination of a bJSF. The correlation assumptions for this category are $\rho_{exp} = \rho_{LHC} = 0$.

uncorrJES: This is the JES uncertainty component which is uncorrelated between experiments ($\rho_{LHC} = 0$). For ATLAS it includes contributions from the limited data sample statistics used to derive the standard jet energy calibrations. In addition, uncertainty contributions from detector-specific components, pile-up suppression techniques, and the presence of close-by jet activity are included in this source (see also Appendix A for a description of the ATLAS uncertainty sub-components). For CMS, this uncertainty source includes the statistical uncertainty of the default jet energy calibration, contributions stemming from the jet energy correction due to pile-up effects, uncertainties due to the variations of the calorimeter response versus time, and finally detector specific effects. This uncertainty category is fully correlated between measurements from the same experiment ($\rho_{exp} = 1$).

in-situγ/ZJES: This corresponds to the part of the JES uncertainty stemming from modelling uncertainties affecting the absolute JES determination using γ/Z+jets events, not included in the previous category. This uncertainty class is fully correlated between measurements from the same experiments, and

Uncertainty Categories			Size [GeV]						Correlation	
			ATLAS		CMS			LHC	ρ_{exp}	ρ_{LHC}
Tevatron	ATLAS	CMS	2011 l+jets	2011 di-l	2011 l+jets	2011 di-l	2011 all jets	comb		
Measured m_{top}			172.31	173.09	173.49	172.50	173.49	173.29		
	Jet Scale Factor		0.27		0.33					
	bJet Scale Factor		0.67							
iJES	Sum (statistical comp.)		0.72		0.33			0.26	0	0
dJES	uncorrelated JES comp.		0.61	0.73	0.24	0.69	0.69	0.29	1	0
dJES	in-situ γ/Z JES comp.		0.29	0.31	0.02	0.35	0.35	0.10	1	0
dJES	intercalib. JES comp.		0.19	0.39	0.01	0.08	0.08	0.07	1	0.5
aJES	flavour JES comp.		0.36	0.02	0.11	0.58	0.58	0.16	1	0.0
bJES	b-jet energy scale		0.08	0.71	0.61	0.76	0.49	0.43	1	0.5
Signal	MC Generator		0.19	0.20	0.02	0.04	0.19			
Signal	Hadronisation		0.27	0.44						
Signal: MC	Sum		0.33	0.48	0.02	0.04	0.19	0.14	1	1
Signal	ISR/FSR		0.45	0.37						
Signal		Q^2-scale			0.24	0.55	0.22			
Signal		Jet-Parton scale			0.18	0.19	0.24			
Signal: Rad	Sum		0.45	0.37	0.30	0.58	0.33	0.32	1	1
Signal: CR	Colour reconnection		0.32	0.29	0.54	0.13	0.15	0.43	1	1
Signal: -	Underlying event		0.12	0.42	0.15	0.05	0.20	0.17	1	1
Signal: PDF	Proton PDF		0.17	0.12	0.07	0.09	0.06	0.09	1	1
	Jet Resolution		0.22	0.21	0.23	0.14	0.15			
	Jet Reco Efficiency		0.05							
	E_T^{miss}		0.03	0.05	0.06	0.12				
DetMod	Sum		0.23	0.22	0.24	0.18	0.28	0.20	1	0
	b-tagging		0.81	0.46	0.12	0.09	0.06	0.25	1	0.5
LepPt	Lepton reconstruction		0.04	0.12	0.02	0.14		0.01	1	0
Background from MC				0.14	0.13	0.05		0.08	1	1
Background from Data			0.10				0.13	0.04	0	0
Method			0.13	0.07	0.06	0.40	0.13	0.06	0	0
Multiple Hadronic Interactions			0.03	0.01	0.07	0.11	0.06	0.05	1	1
Statistics			0.23	0.64	0.27	0.43	0.69	0.23		
Systematics			1.53	1.50	1.03	1.46	1.23	0.92		
Total Uncertainty			1.55	1.63	1.06	1.52	1.41	0.95		
Comb. Coeff. [%]			22.6	3.6	60.6	-8.4	21.6	χ^2/ndf = 1.8/4		
Pull			-0.80	-0.15	0.41	-0.67	0.19	χ^2 prob = 77%		

Table 1: Uncertainty categories mapping for the input measurements and the result of the LHC m_{top} combination. For comparison, the categorisation used in the Tevatron 2013 combination [2] is reported in the first column. The correlation ρ_{exp} represents the assumed correlation between measurements from the same experiment, while ρ_{LHC} indicates the correlation assumed between measurements across experiments. The values of ρ_{exp} and ρ_{LHC} are reported for the categorisation actually used in the combination, and are omitted for those sub-categories which are grouped into a single uncertainty component. The stability of the result under different correlation assumptions is discussed in Section 6.

it is assumed to be uncorrelated between ATLAS and CMS measurements: $\rho_{exp} = 1$; $\rho_{LHC} = 0$. Since the methodologies and assumptions to derive corrections and uncertainties are not always directly comparable between the two experiments, variations of ρ_{LHC} are considered in the combination stability checks.

intercalibJES: This is the JES uncertainty component originating from the modelling of the radiation in the relative jet η (central-forward) and p_{T} inter-calibration procedures. Within CMS, when evaluating this uncertainty contribution, an extrapolation to zero radiation is performed, and sizable statistical contributions are present. As a result, the combination is carried out with $\rho_{exp} = 1; \rho_{LHC} = 0.5$, and variations of these assumptions are monitored by performing stability checks.

flavourJES: This includes the part of the JES uncertainty stemming from differences in the jet energy response for various jet flavours (quark- versus gluon-originated jets) and flavour mixture, with respect to those used in the calibration procedures. Contributions stemming from the modelling of b-quark jets are treated separately and included in the following uncertainty category. The m_{top} combined result is obtained with $\rho_{exp} = 1; \rho_{LHC} = 0$, and as in the previous cases, variations of ρ_{LHC} are analysed.

bJES: This accounts for an additional b-jet specific uncertainty, arising from the uncertainty in the modelling of the response of jets originating from b-quarks [20, 21]. In ATLAS, this uncertainty covers the effects stemming from b-quark fragmentation, hadronisation and underlying soft radiation and it is determined using different Monte Carlo event generation models [20]. For the ATLAS $t\bar{t} \to$ lepton+jets input measurement [4], due to the simultaneous fit of the m_{top} together with a JSF and a bJSF, the impact of this uncertainty is reduced to 0.08 GeV, albeit at the cost of an additional statistical component in the iJES class, which, with the present integrated luminosity, amounts to 0.67 GeV. For CMS the bJES is defined as the full "flavour-dependent" uncertainty on the difference in the response between light-quark and gluon originated jets. This uncertainty class is assumed to be fully correlated between measurements from the same experiments, and partially correlated across experiments ($\rho_{LHC} = 0.5$) because of the different methods used to evaluate it (see also Section 6). Stability checks are performed changing the value of ρ_{LHC} to unity.

In the current LHC combination, the component of the systematic uncertainty stemming from the modelling of signal events is divided into several sub-categories, assumed to be fully correlated between measurements from the same experiments ($\rho_{exp} = 1$), and across experiments ($\rho_{LHC} = 1$):

MC: (Monte Carlo) This sub-category includes uncertainties stemming from the choice of the Monte Carlo generator. For ATLAS, the systematic uncertainty is calculated comparing m_{top} results obtained with MC@NLO [23, 24] or PowHeg. For CMS, the baseline MadGraph MC setup does not include the simulation of the decay widths of the top-quarks and the W bosons. A systematic uncertainty obtained comparing the m_{top} results in MC samples generated with PowHeg or MadGraph is assigned to also cover this effect. For ATLAS measurements, this uncertainty class includes a contribution due to the choice of the hadronisation model used in the simulation (see also Section 6).

Rad: (Radiation) This category includes uncertainties due to the modelling of QCD radiation in $t\bar{t}$ events. For the ATLAS measurements, variations of initial and final state radiation (ISR/FSR) parameters within Pythia, which are constrained by ATLAS data, are used to evaluate these m_{top} systematic uncertainties. In CMS, where $t\bar{t}$ events are generated using a multi-leg MC, samples with varied factorisation and renormalisation scale (Q^2-scale) and varied minimum p_{T} used in the MLM matching procedure [17] (Jet-Parton scale), are used to address these systematic uncertainties. Investigations from Refs. [25,26] indicate that the two approaches describe to a large extent the same physics effect.

CR: (Colour Reconnection) This is the part of the uncertainty related to the modelling of colour reconnection effects. It is assessed by comparing simulated samples with the hadronisation based on the Pythia tunes Perugia 2011 and Perugia 2011 noCR [15].

UE: (Underlying Event) This category relates to uncertainties in the modelling of the underlying event[1].

[1]It is not quoted as a separate category in the current Tevatron combination [2].

The uncertainty is obtained by comparing simulated samples in which the hadronisation is performed using Pythia with tunes Perugia 2011 and Perugia 2011 mpiHi [15].

PDF: (Parton Distribution Functions) This is the part of the modelling uncertainty related to the proton PDF. It is evaluated by re-weighting the simulated signal events according to the ratio of the default central PDF (CT10 and CTEQ6.6L for ATLAS and CMS, respectively) and the corresponding eigenvector variations [27, 28]. The uncertainty contribution corresponding to the re-weighting of the events to alternative PDF sets is found to be smaller than the above variation and not included.

DetMod: (Detector Modelling) This category relates to uncertainties in the modelling of detector effects. These include uncertainties in the jet energy resolution [21,29], the jet reconstruction efficiency [19] as well as uncertainties related to the missing transverse energy reconstruction, $E_{\mathrm{T}}^{\mathrm{miss}}$ [30,31]. This uncertainty class is assumed to be fully correlated between measurements from the same experiments ($\rho_{exp} = 1$), but uncorrelated across experiments ($\rho_{LHC} = 0$).

b-tag: (b-tagging) This is the part of the uncertainty related to the modelling of the b-tagging efficiency and the light-quark jet rejection factors in the MC simulation with respect to the data [32–35]. The m_{top} combined result is obtained with $\rho_{exp} = 1$ and $\rho_{LHC} = 0.5$ for this systematic source[2], but variations of ρ_{exp}, and ρ_{LHC} are analysed in the stability checks (see Section 6 for further details). Despite the sizable reduction of the bJES related systematics that is achieved, the ATLAS $t\bar{t} \rightarrow$ lepton+jets analysis exhibits an increased sensitivity to the uncertainties of the b-tagging efficiency and of the light jet rejection factors. This is related to the shape differences introduced by the b-tagging scale factor variations in the variable sensitive to the bJSF [4].

LepPt: This category takes into account the uncertainties in the efficiency of the trigger, in the identification and reconstruction of electrons and muons, and residual uncertainties due to a possible miscalibration of the lepton energy and momentum scales [36–38]. The correlation assumptions for this uncertainty source are $\rho_{exp} = 1$, and $\rho_{LHC} = 0$.

BGMC: (Background from MC) This represents the uncertainty due to the modelling of the background normalisation and shape determined from MC. This uncertainty source is assumed to be fully correlated between all measurements ($\rho_{exp} = \rho_{LHC} = 1$).

BGData: (Background from Data) This class includes the uncertainties of the modelling of the background determined from data, and is assumed to be uncorrelated between all input measurements ($\rho_{exp} = \rho_{LHC} = 0$). Typically, these originate from uncertainties in the normalisation of the QCD multijet background.

Method: This systematic uncertainty relates to the fitting technique adopted for the m_{top} measurements (uncorrelated between all measurements: $\rho_{exp} = \rho_{LHC} = 0$). This includes uncertainties caused by the limited MC statistics available for the measurement calibration.

MHI: (Multiple Hadronic Interactions) This systematic uncertainty arises from the modelling of the pile-up conditions in the simulation with respect to the data (overlay of multiple hard proton-proton interactions). It is assumed to be fully correlated between all current input measurements ($\rho_{exp} = \rho_{LHC} = 1$).

[2] Due to the large sensitivity of the ATLAS $t\bar{t} \rightarrow$ lepton+jets analysis to this uncertainty class, $\rho_{LHC} = 0.5$ has been adopted for the default combination, as it is considered to be a more conservative assumption.

5 LHC combination

The methodology, and the information described above, result in the combined LHC m_{top} value of

$$m_{\text{top}} = 173.29 \pm 0.23\ (\text{stat}) \pm 0.92\ (\text{syst})\ \text{GeV}.$$

Alternatively, separating the iJES statistical contribution from the quoted systematic uncertainty, the result reads:

$$m_{\text{top}} = 173.29 \pm 0.23\ (\text{stat}) \pm 0.26\ (\text{iJES}) \pm 0.88\ (\text{syst})\ \text{GeV}.$$

The χ^2 of the combination is 1.8 for 4 degrees of freedom and the corresponding probability is 77%. Its value can be used to assess the extent to which the individual measurements are consistent with the combined m_{top} value and with the hypothesis that they measure the same physics parameter. Moreover, for each input value of the top quark mass, m_i, the pull, defined as: $\text{pull}_i = (m_i - m_{\text{top}})/\sqrt{\sigma^2_{m_i} - \sigma^2_{m_{\text{top}}}}$, where $\sigma_{m_{\text{top}}}$ is the total uncertainty of the combined m_{top} result, indicates a good agreement between all input measurements.

Table 1 and Figure 1 summarise the inputs and the results of the combination. For each measurement, the coefficient (BLUE combination coefficient) used in the linear combination of the input m_{top} values to obtain the combined result, and the pull value are also provided. Within the BLUE method, negative coefficients can occur when combining measurements with different precision and large correlations [11]. The negative BLUE combination coefficient for the CMS $t\bar{t} \to$ di-lepton measurement has been studied by varying the assumptions on the correlations. As expected, if the correlations are artificially reduced all the combination coefficients can become positive.

In Figure 1(a), the combination result and the input measurements are compared with the current Tevatron m_{top} combination [2]. The statistical uncertainty, the iJES contribution (when applicable) and the sum of the remaining uncertainties are reported separately. Figure 1(b) and Figure 1(c) report the BLUE combination coefficients and the pulls of the input measurements with respect to the combined m_{top} result.

Following the proposal and the BLUE software implementation documented in Ref. [39], the impact of the various input measurements is estimated using the Fisher information concept, $I = 1/\sigma^2_{m_{\text{top}}}$. For each of the input measurements, intrinsic (IIW_i) and marginal information weights (MIW_i) are derived. The intrinsic information weight carried by the i^{th}-measurement is complemented by the introduction of a weight inherent to the ensemble of all correlations between the input measurements (IIW_{corr}):

$$\text{IIW}_i = \frac{1/\sigma_i^2}{1/\sigma^2_{m_{\text{top}}}} = \frac{1/\sigma_i^2}{I};\ \ \text{IIW}_{corr} = \frac{I - \sum_i 1/\sigma_i^2}{I}.$$

The IIW_i for each individual measurement is defined as the ratio of the information it carries when taken alone ($1/\sigma_i^2$) to the total information of the combination. While the IIW_i are defined to be positive, IIW_{corr} can be negative, or positive, depending on whether the net effect of the correlations is to increase, or decrease, the total uncertainty of the combination. The marginal information weight defined as

$$\text{MIW}_i = \frac{I_{\text{n. meas}} - I_{\text{n}-1\ \text{meas.: all but}\ i}}{I_{\text{n. meas}}}$$

can also be used to quantify the information that an individual measurement brings in a combination. The MIW_i encodes the additional information available when the i^{th}-measurement is added to a combination that already includes $n - 1$ inputs. It quantifies the relative improvement in the total variance that is achieved by adding the measurement under consideration to the combination of all the others. The intrinsic and marginal information weight, for each individual input measurement, and the intrinsic

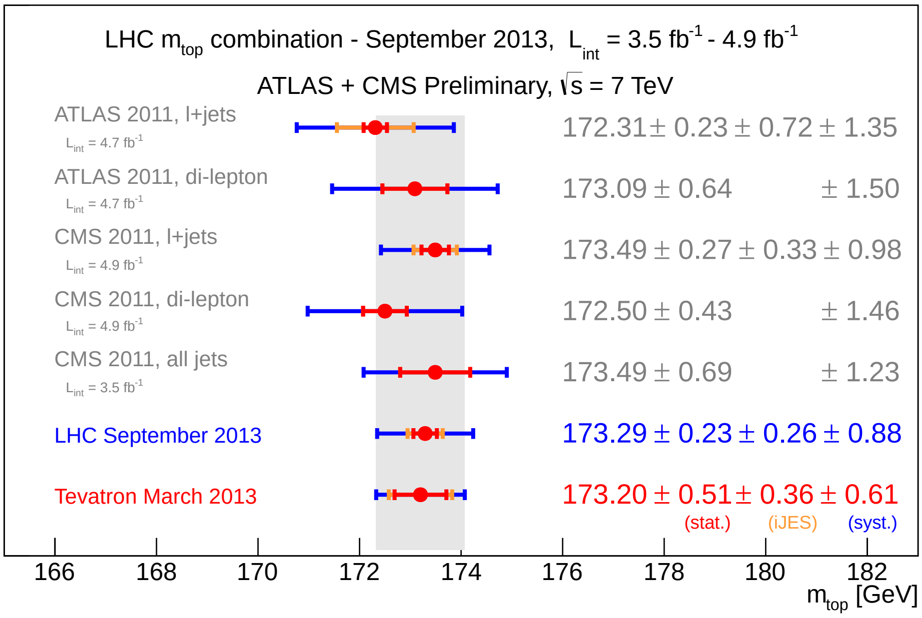

(a)

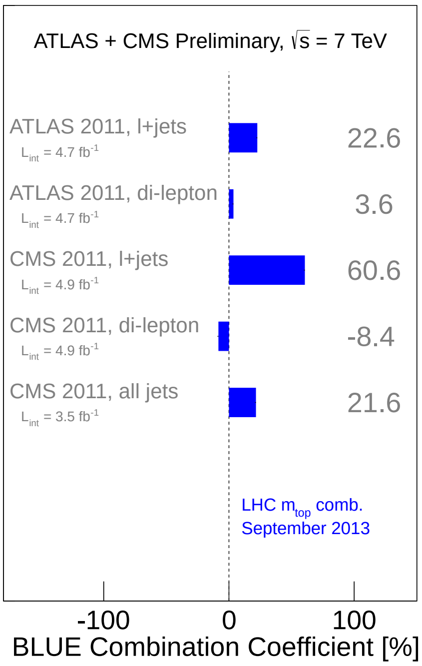

(b)

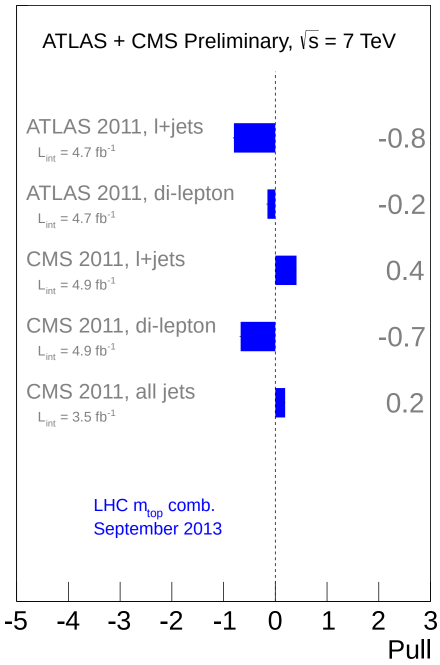

(c)

Figure 1: (a): Input measurements and result of the LHC combination (see also Table 1), compared with the Tevatron combined m_{top} value [2]; for each measurement, the statistical uncertainty, the iJES contribution (when applicable) and the sum of the remaining uncertainties are reported separately. The iJES contribution is statistical in nature and applies to analyses performing in-situ ($t\bar{t}$) jet energy calibration procedures. The grey vertical band indicates the total Tevatron m_{top} uncertainty. (b, c) : BLUE combination coefficients and pulls of the input measurements.

Measurements		BLUE comb. coeff. [%]	IIW [%]	MIW [%]
ATLAS l+jets	172.31 ± 1.55	22.6	37.3	8.2
ATLAS di-l	173.09 ± 1.63	3.6	33.8	0.2
CMS l+jets	173.49 ± 1.06	60.6	79.2	25.1
CMS di-l	172.50 ± 1.52	-8.4	38.8	0.7
CMS all jets	173.49 ± 1.41	21.6	45.0	4.4
Correlations	—	—	−134.1	—

Table 2: Evaluation of the impact of the input measurements in the combination. The following values are listed for each measurement i: the BLUE combination coefficient, the intrinsic information weight IIW_i, and the marginal information weight MIW_i. The intrinsic information weight IIW_{corr} of correlations is also shown on a separate row [39].

information weight of the correlations, are listed in Table 2. For comparison the corresponding BLUE combination coefficients are also reported. The intrinsic information weight carried by the ensemble of the correlations among measurements is large in comparison to the contribution of the individual m_{top} inputs. It is therefore important to monitor the stability of the result under variations of the corresponding assumptions (see Section 6).

The total correlation matrix, $\mathcal{M}_\rho$, of the ATLAS and CMS m_{top} measurements is reported below. The elements in the matrix are labelled according to the analysis they correspond to (rows and columns read as ATLAS or CMS followed by the $t\bar{t}$ decay channel name).

$$\begin{array}{cc} & \begin{array}{ccccc} \text{ATLAS } l\text{+jets} & \text{ATLAS di-}l & \text{CMS } l\text{+jets} & \text{CMS di-}l & \text{CMS all jets} \end{array} \\ \mathcal{M}_\rho \; = & \left(\begin{array}{ccccc} 1.00 & & & & \\ 0.63 & 1.00 & & & \\ 0.26 & 0.35 & 1.00 & & \\ 0.18 & 0.25 & 0.64 & 1.00 & \\ 0.16 & 0.24 & 0.55 & 0.75 & 1.00 \end{array} \right) \begin{array}{l} \text{ATLAS } l\text{+jets} \\ \text{ATLAS di-}l \\ \text{CMS } l\text{+jets} \\ \text{CMS di-}l \\ \text{CMS all jets} \end{array} \end{array}$$

The precision of the combined result with respect to the most precise single measurement is improved by about 10%. The total uncertainty of the combination amounts to 0.95 GeV, and corresponds to a relative uncertainty on m_{top} of 0.5%. The resulting total uncertainty is dominated by the systematic contributions related to the modelling of signal events and the knowledge of the jet energy scale for light- and b-quark originated jets.

Using the same inputs, uncertainty categorisation, and correlation assumptions, the combination has been repeated to determine three correlated m_{top} values for the individual $t\bar{t}$ decay channels ($m^{l\text{+jets}}$, $m^{\text{di-}l}$, $m^{\text{all jets}}$). This is achieved within the BLUE program by simultaneously fitting three mass parameters, one for each channel, instead of a common m_{top}. The consistency between the m_{top} determination in the various channels is measured using the following pair-wise χ^2 formulation and its associated probability: $\chi^2(m_1, m_2) = (m_1 - m_2)^2/\sigma_{12}^2$, where $\sigma_{12}^2 = \sigma_1^2 + \sigma_2^2 - 2\rho_{12}\sigma_1\sigma_2$, and ρ_{12} is the correlation between the two measurements. The results are summarised in Table 3. Due to the correlations between the fitted parameters, the $m^{\text{all jets}}$ does not trivially coincide with the CMS $t\bar{t} \to$ all jets input measurement.

Similarly the combination has been repeated to obtain two correlated m_{top} values for the ATLAS and CMS experiments (m^{ATL}, m^{CMS}). The latter results are compared to the individual combinations of the

	Parameter value	Correlations			χ^2/ndf (χ^2 probability)		
		$m^{l\text{+jets}}$	$m^{\text{di-}l}$	$m^{\text{all jets}}$	$m^{l\text{+jets}}$	$m^{\text{di-}l}$	$m^{\text{all jets}}$
$m^{l\text{+jets}}$	173.18 ± 0.97	1.00			–		
$m^{\text{di-}l}$	172.85 ± 1.24	0.72	1.00		0.15/1 (0.70)	–	
$m^{\text{all jets}}$	173.64 ± 1.30	0.56	0.70	1.00	0.17/1 (0.68)	0.64/1 (0.42)	–

Table 3: Combination results in terms of three physical parameters corresponding to the individual $t\bar{t}$ decay channels. The determination of the m_{top} per decay channel is reported together with the pair-wise correlation coefficients, and the compatibility tests in terms of χ^2/ndf and its associated probability.

	Individual combinations	Parameter value	Correlations		χ^2/ndf (χ^2 probability)	
			m^{ATL}	m^{CMS}	m^{ATL}	m^{CMS}
m^{ATL}	172.65 ± 1.43	172.70 ± 1.43	1.00		–	
m^{CMS}	173.59 ± 1.03	173.50 ± 1.02	0.33	1.00	0.21/1 (0.65)	–

Table 4: Combination results in terms of two physical parameters corresponding to the m_{top} determinations from the individual experiments. The determination of the m_{top} per experiment is reported together with the pair-wise correlation coefficients, and the compatibility tests in terms of χ^2/ndf and its associated probability. For comparison the results of the separate combinations of the individual ATLAS and CMS inputs from Table 1 are reported in the second column.

ATLAS and CMS inputs in Table 4. The full uncertainty breakdown of the separated ATLAS and CMS combinations is reported in Appendix B.

6 Effects of using alternative correlation models and uncertainty treatments

The categorisation and the correlation assumptions summarised in Table 1 reflect the present understanding and the limitations due to the different choices made by the experiments when evaluating the individual uncertainty sources.

Despite the various improvements in the categorisation since the previous LHC combination, and the usage of a finer JES sub-component splitting, the final harmonisation of the methodologies and the uncertainty classes needs further dedicated studies by both experiments. In this preliminary result, the impact of the approximations is evaluated by performing stability cross checks, in which the input assumptions are changed with respect to the values reported in Table 1. The results of these cross checks are described in the following, and summarised in Figure 2.

6.1 Overall correlations

The stability of the combined m_{top} result with respect to the correlation assumptions reported in Table 1, has been checked by changing, simultaneously for all systematic sources, the values of ρ_{exp} and ρ_{LHC} by a multiplicative factor, f, in the range [0, 1]. The result of this stability check in terms of the shifts of the combined m_{top} value (Δm_{top}) and of its total uncertainty ($\Delta\sigma_{m_{\text{top}}}$) are reported in Figure 2(a,b). For the extreme case of no correlation ($f = 0$) the result is $\Delta m_{\text{top}} = -212$ MeV and $\Delta\sigma_{m_{\text{top}}} = -328$ MeV. The sensitivity of the combination to the assumed correlations between measurements from the same experiments, or across experiments, has been evaluated using separate variations of ρ_{exp} and ρ_{LHC}, respectively.

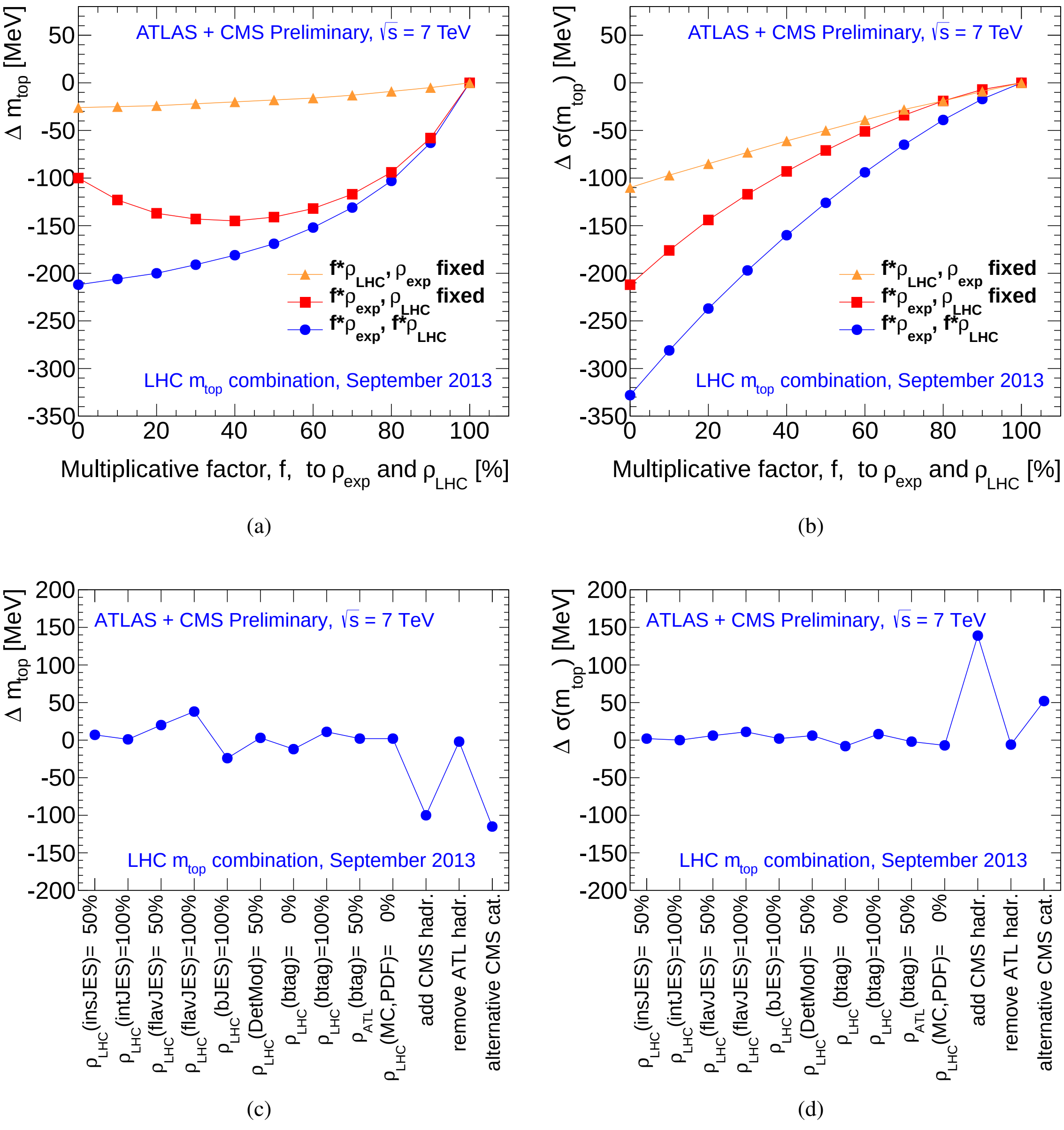

Figure 2: Variation of the combined m_{top} result (a,c) and its total uncertainty (b,d) as a function of variations in the correlation assumptions. (a,b) ρ_{exp} and ρ_{LHC} are varied using a multiplicative factor f in the range [0,1] (blue curve). Separate variations of ρ_{exp} and ρ_{LHC}, in the same range, are reported by the red and the orange curve, respectively. (c,d) Stability of the LHC combination under variations of the default assumptions on ρ_{LHC} and ρ_{exp} for selected uncertainty sources. The sensitivity of the combination to different scenarios concerning the treatment of the hadronisation systematics is also shown.

For the case in which ρ_{LHC} (ρ_{exp}) is varied while keeping ρ_{exp} (ρ_{LHC}) fixed, the maximum observed variations are $\Delta m_{\mathrm{top}} = -26$ MeV and $\Delta\sigma_{m_{\mathrm{top}}} = -110$ MeV ($\Delta m_{\mathrm{top}} = -145$ MeV and $\Delta\sigma_{m_{\mathrm{top}}} = -212$ MeV), signalling a larger sensitivity of the result to the intra-experiment correlations. The separate ρ_{exp} and ρ_{LHC} variations as a function of the value of the multiplicative factor f are reported by the red and the orange curve in Figure 2(a,b), respectively. Studies performed keeping fixed $\rho_{LHC} = 0.5$ instances, and varying $\rho_{LHC} = 1 \to 0$ and $\rho_{exp} = 1 \to 0$, provide similar results.

6.2 JES component correlations

The methodologies and assumptions used to derive the jet energy corrections and the related uncertainties are not always directly comparable between the ATLAS and CMS experiments. As a consequence, variations of the corresponding ρ_{LHC} assumptions, have been considered in the combination stability checks. These affected the in-situ γ/Z ($\rho_{LHC} = 0.5$), inter-calibration ($\rho_{LHC} = 1.0$), and flavour ($\rho_{LHC} = 0.5,\ 1.0$) components of the JES. The maximum deviations observed with respect to the default result are: $\Delta m_{\mathrm{top}} = 38$ MeV and $\Delta\sigma_{m_{\mathrm{top}}} = 11$ MeV.

A different strategy is also followed concerning the evaluation of the b-jet specific energy scale uncertainty. In ATLAS, the effects stemming from b-quark fragmentation, hadronisation and underlying soft radiation are studied using different MC event generation models [20]. On the other hand, in CMS, the Pythia and Herwig [40] fragmentation models are used to evaluate the response variation for different jet flavour mixtures. The inclusive jet flavour mixture and b-jet responses are both well modelled, while the largest differences are found for pure quark and gluon flavours. The maximum of these differences, for pure quark flavour at low p_{T} and for pure gluon flavour at high p_{T}, is taken as a flavour uncertainty applicable to any jet flavour or flavour mixture [21]. To reflect these differences in the estimate of the b-JES uncertainty, $\rho_{LHC} = 0.5$ is used as the default assumption for this source of systematic uncertainty. The changes of the combination when using $\rho_{LHC} = 1$ are studied as another stability test. The results of this are $\Delta m_{\mathrm{top}} \leq 25$ MeV, $\Delta\sigma_{m_{\mathrm{top}}} \leq 5$ MeV.

6.3 Signal modelling

6.3.1 ATLAS and CMS correlation

For the evaluation of the MC systematic uncertainty, different MC generators are used within the ATLAS and CMS collaborations. In addition a contribution to the uncertainty due to the choice of the hadronisation model used in the simulation is included for the ATLAS input measurements. Finally, different input PDF (CT10 and CTEQ6.6L for ATLAS and CMS, respectively) are used in the baseline MC by the two collaborations. These aspects may reduce the actual correlation between ATLAS and CMS measurements for these uncertainty classes. As a result, the combination has been repeated using $\rho_{LHC} = 0$ for both the MC and PDF uncertainty sources: the observed deviations with respect to the default result are $\Delta m_{\mathrm{top}} = 2$ MeV, and $\Delta\sigma_{m_{\mathrm{top}}} = -7$ MeV.

6.3.2 Hadronisation and alternative uncertainty categorisation

As mentioned above, in the signal modelling categorisation, additional uncertainties can arise from the choice of the hadronisation model (cluster or string fragmentation as implemented in Herwig and Pythia, respectively) describing the transition from final state partons to colourless hadrons. The change in m_{top} obtained by exchanging cluster and string models in a fixed MC setup can be quoted as hadronisation uncertainty for the m_{top} measurements. However, this source of uncertainty is typically also considered among the components of the jet energy scale uncertainty (both for inclusive- and b-quark jets) and sizable double counting effects may result. For the time being, the experiments choose different approaches. ATLAS quotes an explicit hadronisation systematic related to the $t\bar{t}$ modelling in the MC. Within CMS, to minimise double counting, no additional hadronisation systematic is quoted. Given the relatively large size of this uncertainty (Table 1), a harmonisation of the treatments of this systematics is needed. Specifically, an in-depth investigation of the level of the double counting effects involved when both types of components are used is important for the next generation of measurements and $m_{\rm top}$ combinations. These studies are currently in progress. To estimate the possible significance of these effects, the LHC $m_{\rm top}$ combination has been repeated for several different assumptions. From the comparison of PowHeg simulations with Pythia and Herwig used for the fragmentation stage, CMS has derived estimates of the hadronisation uncertainty of 0.58, 0.76 and 0.93 GeV for the l+jets, di-l, and all jets channels, respectively. Adding these into the MC systematic uncertainty, and repeating the combination, results in $\Delta m_{\rm top} = -100$ MeV and $\Delta\sigma_{m_{\rm top}} = +139$ MeV. The relatively large effect is introduced by an increased total uncertainty for the CMS input measurements, and the resulting change of the combination coefficients of the measurements in the combination. In this case and for the five input measurements, these read: 29.4%, 5.0%, 64.6%, -6.9%, 7.9%, where the values refer to the ATLAS l+jets and di-l measurements and the CMS l+jets, di-l, and all jets measurements respectively. Alternatively, if the extra hadronisation systematics evaluated by ATLAS in addition to the JES components, is removed, the observed changes are $\Delta m_{\rm top} = -2$ MeV and $\Delta\sigma_{m_{\rm top}} = -6$ MeV. In addition to the above investigations, CMS has studied an alternative systematic categorisation. While keeping the hadronisation uncertainties described above, the bJES uncertainty is evaluated at the analysis level using the uncertainties in the b-fragmentation function, and the b-semileptonic branching fractions. The uncertainty in the b-fragmentation is evaluated by varying the Bowler-Lund parameters used to model the b-quark fragmentation in Pythia between the Pythia Z2 tune and the results of the Perugia P2011 [15] and Corcella [40] tunes. This results in an uncertainty of $m_{\rm top}$ of 0.15 GeV. An additional uncertainty of 0.10 GeV comes from varying the b-semileptonic branching fractions within their measured uncertainties. In this framework, the combined uncertainty of 0.18 GeV is taken as the bJES uncertainty for all CMS input measurements. The impact of changing to this characterisation of the hadronisation and bJES uncertainties for the CMS analyses is found to be $\Delta m_{\rm top} = -115$ MeV and $\Delta\sigma_{m_{\rm top}} = +52$ MeV. Further work is needed to resolve this issue and detailed studies are ongoing.

Due to the sensitivity of the combined result to the treatment of hadronisation uncertainties, progress on these aspects will be of key importance for future analyses of increased precision, and for LHC $m_{\rm top}$ combination updates.

6.4 Detector modelling correlations

The detector modelling systematics could include some level of correlation between experiments introduced by the use of MC simulation in the evaluation of the detector performances. For this reason, a test is performed varying the default ρ_{LHC} from 0% to 50%. The impact of this change is found to be $\Delta m_{\rm top} = 3$ MeV and $\Delta\sigma_{m_{\rm top}} = 6$ MeV.

In the evaluation of the b-tagging uncertainties affecting the $m_{\rm top}$ measurements, data-to-MC scale factors (SF), to adjust the b-tagging performance in the simulation, are varied within their uncertainty. These are derived as functions of the jet flavour and the jet properties. In ATLAS, the full $p_{\rm T}/\eta$ dependency on the SF is taken into account. On the other hand, CMS top-quark mass analyses evaluate this uncertainty by changing the b-tag selection criteria to mimic the b-tagging efficiency variations, but no explicit $p_{\rm T}/\eta$ dependence is currently considered. Due to the large contribution to the total uncertainty from this source, the ATLAS l+jets $m_{\rm top}$ result used SF derived from a combination of the different calibrations obtained from a $t\bar{t} \rightarrow$ di-lepton sample ($t\bar{t}$-based) [33], and a sample of jets including muons (muon-based) [34]. This allowed a reduction of the SF uncertainties as a function of the jet $p_{\rm T}$. The ATLAS $t\bar{t} \rightarrow$ di-lepton measurements used instead muon-based only b-tagging calibrations. For these reasons, the default correlation assumptions $\rho_{exp} = 1.0$ and $\rho_{LHC} = 0.5$ have been varied in the stability checks. In particular, combination tests have been performed with $\rho_{LHC} = 0,\ 1.0$, and $\rho_{ATL} = 0.5$, the latter reducing the assumed correlation between ATLAS measurements. The maximum deviations observed with respect to the default results are: $|\Delta m_{\text{top}}| = 12$ MeV and $|\Delta\sigma_{m_{\text{top}}}| = 8$ MeV.

6.5 Minimisation of the Fisher information

As an additional cross check, the stability of the combination has been verified applying the recipes described in Ref. [39]. Numerical minimisation procedures aimed at reducing the Fisher information of the combination are applied, varying the correlation assumptions by multiplicative factors in three different scenarios. In the simplest case, all correlations are rescaled by the same global factor (minimise by global factor). As a second option, the same rescaling factor is applied to all correlations within each error source (minimise by error source). Finally, an alternative minimisation procedure is performed in which for all error sources the off-diagonal correlations ($\rho_{ij},\ i \neq j$) are rescaled by the same factor (minimise by off-diagonal element). The results of these test are reported in Table 5 and confirm the robustness of the combinations against changes of the correlation assumptions.

Alternative cross checks, as proposed in Ref. [39] and adopted in Ref. [41], have been performed and yield consistent results with respect to the default combination.

Combination	BLUE
Nominal correlations	173.29 ± 0.95
Minimise by global factor	173.29 ± 0.95
Minimise by error source	173.27 ± 0.95
Minimise by off-diagonal element	173.21 ± 0.95

Table 5: Summary of the combinations performed with nominal and modified correlations applying the recipes described in Ref. [39].

7 Conclusion and outlook

A preliminary combination of the ATLAS and CMS top-quark mass measurements using data collected from proton-proton collisions at the centre-of-mass energy $\sqrt{s}$=7 TeV during 2011, including up to 4.9 fb^{-1} of integrated luminosity has been presented. In total three published and two preliminary top-quark mass results are included in the combination.

While taking into account correlations between the measurements, the systematic uncertainties were classified following the categories used in the Tevatron 2013 top-quark mass combination. This will facilitate a future combination of LHC and Tevatron measurements.

The resulting combination, taking into account statistical and systematic uncertainties and their correlations, yields:

$$m_{\text{top}} = 173.29 \pm 0.23\ (\text{stat}) \pm 0.92\ (\text{syst})\ \ \text{GeV},$$

or separating the iJES statistical contribution from the quoted systematic uncertainty:

$$m_{\text{top}} = 173.29 \pm 0.23\ (\text{stat}) \pm 0.26\ (\text{iJES}) \pm 0.88\ (\text{syst})\ \ \text{GeV}.$$

The LHC combination achieves an improvement of the total m_{top} uncertainty of about 10% with respect to the most precise input measurement, and supersedes the one documented in [3]. The total uncertainty of the combination amounts to 0.95 GeV, and is currently dominated by the systematic uncertainties due to the jet calibration, and the signal modelling.

The dependence of the result on the correlation assumptions between measurements from the same experiment and across experiments has been studied, and found to be moderate with respect to the current m_{top} precision.

Updated measurements based on the 2012 LHC proton proton run at $\sqrt{s} = 8$ TeV are being performed. In general, larger datasets potentially allow selection of events in phase-space regions where the detector effects are better understood, and derivation of data-driven constraints on the allowed ranges for the signal modelling parameter variations used in the systematic effects determination. As a consequence, future measurements and combinations, profiting from reduced systematics uncertainties as well as from improved analysis techniques, are expected to substantially increase the precision on m_{top} compared to the preliminary results presented here.

A Mapping of LHC and ATLAS jet energy scale categories

In this appendix the grouping of the original ATLAS JES uncertainty categories to those used in the present combination is described. The full JES uncertainty breakdown for the ATLAS input measurements is taken from [4,5]. All sub-components are assumed to be uncorrelated. For further details see also Ref. [19].

ATLAS Component	LHC grouping
Statistical	
Statistical NP1	uncorr. JES comp.
Statistical NP2	uncorr. JES comp.
Statistical NP3	uncorr. JES comp.
Eta intercalibration (statistical)	uncorr. JES comp.
Modelling	
Modelling NP1	in-situ JES comp.
Modelling NP2	in-situ JES comp.
Modelling NP3	in-situ JES comp.
Modelling NP4	in-situ JES comp.
Eta intercalibration (modelling)	intercalib JES comp.
Detector	
Detector NP1	uncorr. JES comp.
Detector NP2	uncorr. JES comp.
Mixed	
Mixed NP1	uncorr. JES comp.
Mixed NP2	uncorr. JES comp.
Single particle high p_{T}	uncorr. JES comp.
Relative non-closure MC	uncorr. JES comp.
Pile-up offset	
Pile-up offset (NPV term)	uncorr. JES comp.
Pile-up offset (μ term)	uncorr. JES comp.
Close-by jets	uncorr. JES comp.
Flavour	
Flavour composition	flavour JES comp.
Flavour response	flavour JES comp.
bJES uncertainty	*b*-JES comp.

Table 6: Grouping of the original ATLAS JES uncertainty categories to those used in the present combination.

B Results of the individual ATLAS and CMS combinations

In this Appendix the separate ATLAS and CMS m_{top} combinations using the same inputs, uncertainty categories, and correlation assumptions as for the LHC m_{top} combination are reported.

	ATLAS comb.	CMS comb.	LHC comb.
Measured m_{top}	172.65	173.59	173.29
iJES	0.41	0.27	0.26
uncorrelated JES comp.	0.66	0.32	0.29
in-situ JES comp.	0.30	0.08	0.10
intercalib. JES comp.	0.28	0.02	0.07
flavour JES comp.	0.21	0.19	0.16
b-jet energy scale	0.35	0.56	0.43
Monte Carlo simulation	0.40	0.06	0.14
Radiation modelling	0.42	0.28	0.32
Colour reconnection	0.31	0.48	0.43
Underlying event	0.25	0.17	0.17
Proton PDF	0.15	0.07	0.09
Detector modelling	0.22	0.25	0.20
b-tagging	0.66	0.11	0.25
Lepton reconstruction	0.07	0.00	0.01
Background from MC	0.06	0.10	0.08
Background from Data	0.06	0.03	0.04
Method	0.08	0.07	0.06
Multiple Hadronic Interactions	0.02	0.06	0.05
Statistics	0.31	0.29	0.23
Systematics	1.40	0.99	0.92
Total Uncertainty	1.43	1.03	0.95

Table 7: Results of the individual ATLAS and CMS combinations using the same inputs listed in Table 1. The uncertainty breakdown is provided and compared with the results of the LHC combination.

References

[1] ALEPH, CDF, D0, DELPHI, L3, OPAL, SLD Collaborations, the LEP Electroweak Working Group, the Tevatron Electroweak Working Group, and the SLD Electroweak and Heavy Flavour Groups, *Precision electroweak measurements and constraints on the Standard Model*, `arXiv:1012.2367 [hep-ex]`.

[2] Tevatron Electroweak Working Group, *Combination of CDF and D0 results on the mass of the top quark using ups to 8.7* fb^{-1} *at the Tevatron*, `arXiv:1305.3929 [hep-ex]`.

[3] ATLAS and CMS Collaborations, *Combination of ATLAS and CMS results on the mass of the top quark using up to 4.9* fb^{-1} *of data*, conference notes CMS-PAS-TOP-12-001 and ATLAS-CONF-2012-095, 2012. `http://cdsweb.cern.ch/record/1460441`.

[4] ATLAS Collaboration, *Measurement of the Top Quark Mass from* $\sqrt{s}$ *= 7 TeV ATLAS Data using a 3-dimensional Template Fit*, conference note ATLAS-CONF-2013-046, 2013. `http://cdsweb.cern.ch/record/1547327`.

[5] ATLAS Collaboration, *Measurement of the Top Quark Mass in Dileptonic Top Quark Pair Decays with* $\sqrt{s}$ *=7 TeV ATLAS Data*, conference note ATLAS-CONF-2013-077, 2013. `http://cds.cern.ch/record/1562935`.

[6] CMS Collaboration, *Measurement of the top-quark mass in $t\bar{t}$ events with lepton+jets final states in pp collisions at $\sqrt{s}$ = 7 TeV*, JHEP **12** (2012) 105, `arXiv:1209.2319 [hep-ex]`.

[7] CMS Collaboration, *Measurement of the top-quark mass in $t\bar{t}$ events with dilepton final states in pp collisions at $\sqrt{s}$ = 7 TeV*, Eur. Phys. J. **C72** (2012) 2202, `arXiv:1209.2393 [hep-ex]`.

[8] CMS Collaboration, *Measurement of the top quark mass in the all-jets final states*, `arXiv:1307.4617 [hep-ex]`. Accepted by Eur. Phys. J. C.

[9] CMS Collaboration, *Measurement of the mass of the $t\bar{t}$ system by kinematic endpoints in pp collisions at $\sqrt{s}$ = 7 TeV*, Eur. Phys. J. C. **73** (2013) 2494, `arXiv:1304.5783 [hep-ex]`.

[10] CMS Collaboration, *Measurement of the top-quark mass using the B-hadron lifetime technique*, conference note CMS-PAS-TOP-12-030, 2013. `https://cds.cern.ch/record/1563140`.

[11] L. Lyons, D. Gibaut, and P. Clifford, *How to combine correlated estimates of a single physical quantity*, Nucl. Instrum. Meth. **A270** (1988) 110.

[12] A. Valassi, *Combining correlated measurements of several different physical quantities*, Nucl. Instrum. Meth. **A500** (2003) 391.

[13] S. Frixione, P. Nason, and C. Oleari, *Matching NLO QCD computations with parton shower simulations: the POWHEG method*, JHEP **11** (2007) 070, `arXiv:0709.2092 [hep-ph]`.

[14] T. Sjostrand, S. Mrenna, and P. Skands, *Pythia 6.4 physics and manual*, JHEP **05** (2006) 026, `arXiv:0603175 [hep-ph]`.

[15] P. Skands, *Tuning Monte Carlo Generators: The Perugia Tunes*, Phys. Rev. D **82** (2010) 074018, `arXiv:1005.3457 [hep-ph]`.

[16] J. Alwall et al., *MadGraph 5: going beyond*, JHEP **06** (2011) 128, `arXiv:1106.0522 [hep-ph]`.

[17] L. Mangano, M. Moretti, and F. Piccinini, *Matching matrix elements and shower evolution for top-pair production in hadronic collisions*, JHEP **01** (2007) 013, `arXiv:0611129 [hep-ph]`.

[18] A. Buckley et al., *General-purpose event generators for LHC physics*, Phys. Rept. **504** (2011) 145, `arXiv:1101.2599 [hep-ph]`.

[19] ATLAS Collaboration, *Jet energy scale and its systematic uncertainty in proton-proton collisions at $\sqrt{s}$ =7 TeV with ATLAS 2011 data*, conference note ATLAS-CONF-2013-004, 2013. `http://cdsweb.cern.ch/record/1509552`.

[20] ATLAS Collaboration, *Jet energy measurement for inclusive jets and b-quark induced jets*, conference note ATLAS-CONF-2013-002, 2013. `http://cdsweb.cern.ch/record/1504739`.

[21] CMS Collaboration, *Determination of Jet Energy Calibration and Transverse Momentum Resolution in CMS*, J. Instrum. **6** (2011) P11002, `arXiv:1107.4277 [hep-ex]`.

[22] CMS Collaboration, *Jet Energy Scale performance in 2011*, CMS DP CMS-DP-2012-006, 2012.

[23] S. Frixione, B. R. Webber, and P. Nason, *MC@NLO Generator version 3.4*, (2002) , `arXiv:0204244 and 0305252 [hep-ph]`.

[24] S. Frixione, P. Nason and B.R. Webber, *Matching NLO QCD and parton showers in heavy flavour production*, JHEP **08** (2003) 007, `arXiv:0305252 [hep-ph]`.

[25] ATLAS Collaboration, *Measurement of ttbar production with a veto on additional central jet activity in pp collisions at $\sqrt{s}$ = 7 TeV using the ATLAS detector*, Eur. Phy. J. **C72** (2012) 2043, arXiv:1203.5015 [hep-ex].

[26] CMS Collaboration, *Measurement of jet multiplicity in di-leptonic top pair events*, conference note CMS-PAS-TOP-12-023, 2012. https://cds.cern.ch/record/1478672.

[27] J. Pumplin et al., *New generation of parton distributions with uncertainties from global QCD analysis*, JHEP **07** (2002) 012, arXiv:0201195 [hep-ph].

[28] M. Botje et al., *The PDF4LHC Working Group Interim Recommendations*, arXiv:1101.0538 [physics.data-an].

[29] ATLAS Collaboration, *Jet energy resolution in proton-proton collisions at $\sqrt{s}$ = 7 TeV recorded in 2010 with the ATLAS detector*, Eur. Phy. J. C. **3** (2013) 2306, arXiv:1210.6210 [hep-ex].

[30] ATLAS Collaboration, *Performance of missing transverse momentum reconstruction in proton-proton collisions at srqrts = 7 TeV with ATLAS*, Eur. Phy. J. **C72** (2012) 1844, arXiv:1108.5602 [hep-ex].

[31] CMS Collaboration, *Missing transverse energy performance of the CMS detector*, J. Instrum. **6** (2011) P09001, arXiv:1106.5048 [hep-ex].

[32] ATLAS Collaboration, *Measuring the mistag rate with 5 fb^{-1} of data from the ATLAS detector*, conference note ATLAS-CONF-2012-040, 2012. http://cds.cern.ch/record/1435194.

[33] ATLAS Collaboration, *Measuring the b-tag efficiency in a ttbar sample with 4.7 fb^{-1} of data from the ATLAS detector*, conference note ATLAS-CONF-2012-097, 2012. http://cds.cern.ch/record/1460443.

[34] ATLAS Collaboration, *Measuring the b-tag efficiency in a sample of jets containing muons with 5 fb^{-1} of data from the ATLAS detector*, conference note ATLAS-CONF-2012-043, 2012. http://cds.cern.ch/record/1435197.

[35] CMS Collaboration, *Commissioning of b-jet identification with pp collisions at sqrt(s) = 7 TeV*, conference note CMS-PAS-BTV-10-001, 2010. http://cdsweb.cern.ch/record/1279144/.

[36] ATLAS Collaboration, *Electron performance measurements with the ATLAS detector using the 2010 LHC proton-proton collision data*, Eur. Phys. J **C72** (2012) 1909, arXiv:1110.3174v2 [hep-ph].

[37] ATLAS Collaboration, *Muon Momentum Resolution in First Pass Reconstruction of pp Collision Data Recorded by ATLAS in 2010*, conference note ATLAS-CONF-2011-046, 2011. https://cdsweb.cern.ch/record/1338575.

[38] CMS Collaboration, *Performance of CMS muon reconstruction in pp collision events at sqrt(s) = 7 TeV*, JINST **7** (2012) P10002, arXiv:1206.4071v1 [hep-ph].

[39] A. Valassi and R. Chierici, *Information and treatment of unknown correlations in the combination of measurements using the BLUE method*, arXiv:1307.4003 [physics.data-an].

[40] G. Corcella et al., *HERWIG 6.5: an event generator for Hadron Emission Reactions With Interfering Gluons (including supersymmetric processes)*, JHEP **01** (2001) 010, arXiv:0011363 [hep-ph].

[41] CMS Collaborations, *Combination of the CMS measurements of the top quark mass based on data recorded between 2010 and 2012*, conference note CMS-PAS-TOP-13-002, 2013. http://cds.cern.ch/record/1599576.